

LLM4GEN: Leveraging Semantic Representation of LLMs for Text-to-Image Generation

Mushui Liu*
lms@zju.edu.cn
Zhejiang University

Yuhang Ma*
yuhang_ma0307@163.com
Fuxi AI Lab, Netease Inc.

Xinfeng Zhang
Fuxi AI Lab, Netease Inc.

Zhen Yang
zheny.cs@zju.edu.cn
Zhejiang University

Zeng Zhao
hzzhaozeng@corp.netease.com
Fuxi AI Lab, Netease Inc.

Zhipeng Hu
Fuxi AI Lab, Netease Inc.

Bai Liu
Fuxi AI Lab, Netease Inc.

Changjie Fan
Fuxi AI Lab, Netease Inc.



Figure 1: Image generation comparison using short and dense prompts across SDXL [31], Playground v2 [19], PixArt- α [8], and our proposed LLM4GEN_{SDXL}. The colored text denotes critical entities or attributes.

ABSTRACT

Diffusion Models have exhibited substantial success in text-to-image generation. However, they often encounter challenges when dealing with complex and dense prompts that involve multiple objects, attribute binding, and long descriptions. This paper proposes a framework called **LLM4GEN**, which enhances the semantic understanding ability of text-to-image diffusion models by leveraging the semantic representation of Large Language Models (LLMs). Through a specially designed Cross-Adapter Module (CAM) that combines the original text features of text-to-image models with LLM features, LLM4GEN can be easily incorporated into various diffusion models as a plug-and-play component and enhances text-to-image generation. Additionally, to facilitate the complex and dense prompts semantic understanding, we develop a LAION-refined

dataset, consisting of 1 million (M) text-image pairs with improved image descriptions. We also introduce DensePrompts which contains 7,000 dense prompts to provide a comprehensive evaluation for the text-to-image generation task. With just 10% of the training data required by recent ELLA, LLM4GEN significantly improves the semantic alignment of SD1.5 and SDXL, demonstrating increases of 7.69% and 9.60% in color on T2I-CompBench, respectively. The extensive experiments on DensePrompts also demonstrate that LLM4GEN surpasses existing state-of-the-art models in terms of sample quality, image-text alignment, and human evaluation. The project website is at: <https://xiaobul.github.io/LLM4GEN/>

KEYWORDS

Text-to-Image Diffusion Models, Large Language Models, Text-Image Alignment

*Equal Contribution.

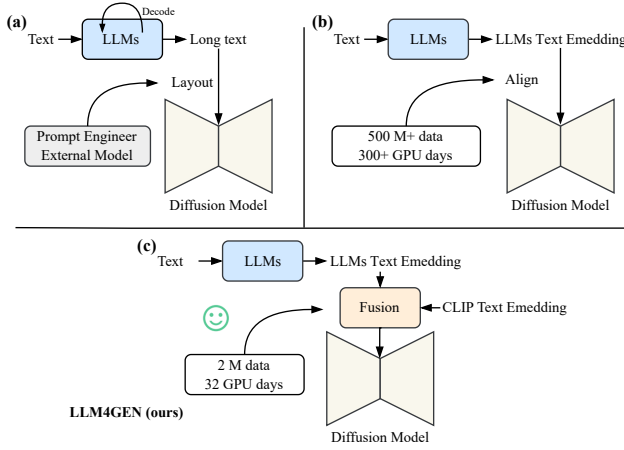


Figure 2: Architecture comparison between (a) LLM-guidance models [23, 55], (b) LLM-alignment models [15, 54], and (c) our proposed LLM4GEN.

1 INTRODUCTION

Recently, diffusion models [7, 10, 17, 43, 47, 56] have made significant progress in text-to-image generation models, such as Imagen [38], DALL-E 2/3 [3, 34], and Stable Diffusion [31, 35]. However, they often encounter challenges in generating images given complex and dense prompt descriptions, such as attribute binding, orientation descriptions, and multiple objects. These limitations may stem from restrictions within the parameters and structure of the text encoder [16].

With the emergence of powerful linguistic representations from Large Language Models (LLMs), there has been an increasing trend in leveraging LLMs to aid in text-to-image generation. Current methods mainly consist of two categories: LLM-guidance models [11, 55] and LLM-alignment models [15, 38, 54]. LLM-guidance models aim to harness the robust encoding and decoding capabilities of LLMs and external models, such as the Layout model, to enhance the representation of text embeddings, subsequently generating images, as illustrated in Fig. 2 (a). However, these methods necessitate the separation of LLMs and external models from the text-to-image models, resulting in redundancy in both inference time and framework. While LLM-alignment models utilize LLMs instead of the vanilla text encoder to capitalize on their superior representational power. This strategy requires a substantial amount of training data to align the representation of LLMs with the diffusion model, imposing a redundant cost on training resources and time, as depicted in Fig. 2 (b).

To tackle the aforementioned challenges, we propose an end-to-end text-to-image framework named **LLM4GEN**, implicitly harnessing the powerful semantic representations of **LLMs** to bolster the representation of the original text encoder **for** text-to-image **GENeration**, as depicted in Fig. 2 (c). Specifically, we design an efficient Cross-Adapter Module (CAM) to implicitly integrate the semantic representation of LLMs with original text encoders that have limited representational capabilities, such as CLIP text encoder [32]. We apply cross-attention on the representation of both encoder-only and decoder-only LLMs, e.g. Llama [60] and T5 [33],

alongside CLIP text embedding, and then concatenate the fused text embedding with CLIP text embedding. The utilization of our CAM substantially improves the performance of text-to-image diffusion models, regardless of whether encoder-only or decoder-only LLMs are used. Furthermore, it preserves the representations produced by original text encoders, thereby diminishing the requirement for extensive training data. Our designed LLM4GEN can be seamlessly integrated into existing diffusion models like SD1.5 [35] and SDXL [31]. As evidenced in Fig. 1, our proposed method exhibits strong performance in text-to-image generation.

To comprehensively assess the image generation capabilities of text-to-image models, we develop a comprehensive benchmark named **DensePrompts**, an extension of T2I-CompBench [16], which incorporates over 7,000 compositional prompts. The construction of this benchmark involves leveraging LLMs for complex text descriptions, followed by manual refinement. Results from performance metrics and human evaluations consistently demonstrate that LLM4GEN’s representational capability surpasses other existing methods. Additionally, we introduce a **LAION-refined dataset**, which is a subset of the open-source LAION [42] dataset, comprising 1M text-image pairs with refined image descriptions. Both the DensePrompts and LAION-refined dataset will be available to the community for further research.

Overall, our contributions are as follows:

- We propose an end-to-end text-to-image framework called LLM4GEN to enhance the text-to-image alignment of diffusion models.
- We introduce a simple but efficient Cross-Adapter Module that integrates robust representation of LLMs into original text encoders that have limited representational capabilities, thereby enhancing semantic understanding for diffusion models.
- We introduce DensePrompts, a comprehensive evaluation benchmark for text-to-image generation, and LAION-refined dataset, a meticulously curated training dataset.
- Experiments show that LLM4GEN exhibits superior performance in sample quality, image-text alignment, and human evaluation compared with existing state-of-the-art models.

2 RELATED WORK

2.1 Large Language Models

Large language models (LLMs) [5] have shown powerful generalization ability in various NLP tasks, e.g., text generation, question answering. LLMs are built on the transformer [52] architecture and guided by the scaling law. Recent LLMs, e.g., GPTs [4], LLaMA [50], OPT [61], BLOOM [40], GLM [58], PaLM [9] are all equipped with billions of parameters, enabling the intriguing capability for in-context learning and demonstrating excellent zero-shot performance across various tasks. Certain Multi-modal LLMs (MLLMs) [1, 2, 53, 62] have effectively integrated LLMs with other modalities, e.g., visual and audio, facilitating more intelligent interactions through the assistance of LLMs. BLIPs [20, 21], LLaVA [25] enhance the synergy of visual understanding and language processing by projecting the visual output to the input layer of LLMs. [30] shows that the frozen LLMs can further integrate visual understanding.

For the text-to-image generation, recent works [18, 23, 48, 55] utilize LLMs to generate the refined text prompts or bounding box layouts [22] for high-quality image generation. However, these existing works only consider LLMs as a simple condition generator, e.g., text prompts or layout planning. In this paper, we harness the representation capabilities of LLMs to enhance text-to-image generation, underscoring the significance of their representational power beyond simple text output.

2.2 Text-to-Image Diffusion Models

Text-to-image generation aims to create images based on given textual descriptions. The diffusion-based models [13, 43, 45–47] have demonstrated remarkable performance in image generation, providing enhanced stability and controllability. These models employ a forward process by adding Gaussian noise to input images and can generate high-quality images with intricate details and diversity through an inverse process from random Gaussian noise. GLIDE [28] and Imagen [38] utilize CLIP [32] text encoder to enhance the image-text alignment. Latent Diffusion Models (LDMs) [35] have been proposed to transfer the diffusion process from pixel to latent space, improving efficiency and image quality. Recent models such as SD-XL [31], DALL-E 3 [3], and Dreambooth [37] have significantly enhanced image quality and text-image alignment using various perspectives, such as training strategies and scaling training data. Despite these notable advancements, generating high-fidelity images aligned with complex and dense textual prompts remains challenging. In this paper, we propose LLM4GEN that implicitly leverages the robust representation capabilities of LLMs to facilitate image generation from textual descriptions.

3 METHOD

3.1 Preliminaries

Diffusion models convert standard Gaussian noise into realistic images through two processes: the forward process and the reverse process [13]. In the forward process, Gaussian noise is gradually added to the data $x_0 \sim q(x_0)$ to obtain a Gaussian distribution with T steps. The reverse process aims to generate the data from an initial Gaussian noise as follows [13]:

$$p_\theta(x_{t-1}|x_t) = \mathcal{N}(x_{t-1}; \mu_\theta(x_t, t), \Sigma_\theta(x_t, t)) \quad (1)$$

where μ_θ can be obtained by predicting the Gaussian noise $z(x_t, t)$ as follows:[13]

$$\mu_0(x_t|t) = \frac{1}{\sqrt{a_t}}(x_t - \frac{\beta_t}{\sqrt{1-a_t}}\epsilon_\theta(x_t, t)) \quad (2)$$

where $\epsilon(x_t)$ is the noise added by the forward process predicted by the neural network.

Conditional diffusion models[14] can be guided in classifier-free guidance, which replaces the explicit classifier with an implicit classifier that does not require calculating the explicit classifier and its gradient. By using classifier-free guidance, the predicted noise can be described as[13]:

$$\bar{\epsilon}_\theta(x_t, t, y) = (\omega + 1)\epsilon_\theta(x_t, t, y) - \omega\epsilon_\theta(x_t, t) \quad (3)$$

where ω is the guidance scale, y is the condition added to guide the diffusion model.

Our work utilizes latent diffusion models (LDMs)[35], consisting of three components: a text encoder such as CLIP[32] for extracting text embeddings, a variational autoencoder (VAE)[51] with an encoder \mathcal{E} to encode images into a low-dimensional latent space, and a decoder \mathcal{D} to reconstruct images from the encoded latent vectors, and a UNet for predicting noise during the diffusion process. The encoder \mathcal{E} maps the input image to the latent space z_t , which is efficient and low-dimensional. The underlying UNet[36] is constructed using 2D convolutional layers and reweighted bounds to focus on the most perceptually relevant features, as follows:

$$L_{LDM} := \mathbb{E}_{\mathcal{E}(x), \epsilon \sim \mathcal{N}(0,1), t} [\|\epsilon - \epsilon_\theta(z_t, t)\|_2^2] \quad (4)$$

where z_t can be obtained from the encoder \mathcal{E} , and latent vectors from $p(z)$ can be decoded to images through the decoder \mathcal{D} . In this paper, we address the limited representation of CLIP as a text encoder by leveraging the capabilities of large language models (LLMs) to enhance the text encoder of the LDMs.

3.2 LLM4GEN

3.2.1 Framework. The proposed LLM4GEN, which contains a Cross-Adapter Module (CAM) and the UNet, is illustrated in Fig. 3 (a). In this paper, we explore stable diffusion [31, 35] as the base text-to-image diffusion model, and the vanilla text encoder is from CLIP [32]. LLM4GEN leverages the strong capability of LLMs to assist in text-to-image generation. The CAM extracts the representation of a given prompt via the combination of LLM and CLIP text encoder. The fused text embedding is enhanced by leveraging the pre-trained knowledge of LLMs through the simple yet effective CAM. By feeding the fused text embedding, LLM4GEN iteratively denoises the latent vectors with the UNet and decodes the final vector into an image with the VAE.

3.2.2 Cross-Adapter Module. The CAM connects the LLMs and the CLIP text encoder using a cross-attention layer, followed by concatenation with the representation of the CLIP text encoder. The last hidden state of the LLMs is extracted as LLMs feature c_l . The feature of CLIP text encoder is denoted as c_t , and we perform a cross-attention to fuse them:

$$Q = W_q(c_l), K = W_k(c_t), V = W_v(c_t) \quad (5)$$

$$c'_l = \text{CrossAttention}(Q, K, V) = \text{softmax}(Q \cdot K^T) \cdot V \quad (6)$$

where W_q, W_k, W_v are the trainable linear projection layers. The output embedding dimension is the same as that of CLIP text encoder. Then the final fused text embedding of the CAM is:

$$c'_t = \text{Concat}(\lambda * c'_l, c_t) \quad (7)$$

where the Concat denotes concatenation in the sequence dimension, and λ is the balance factor.

Then, we feed c'_t into the UNet:

$$x = \text{CA}(x, c'_t) = \lambda * \text{CA}(x, c_l) + \text{CA}(x, c_t) \quad (8)$$

where x denotes the latent noise, CA is the cross-attention module within the UNet module, which receives z as the query and c'_t as the key and value.

Overall, our designed Cross-Adapter Module implicitly facilitates the strong representation of LLMs with a residual fusion manner, without utilizing extensive training data and resources to condition



Figure 3: The overview of LLM4GEN. (a) The inference pipeline. (b) Cross-Adapter Module.

Algorithm 1 LLM4GEN Pipeline

- 1: **Input:** Pretrained UNet ϵ , pre-trained text encoder T_ϕ , pre-trained LLM T_L , Cross-Adapter Module M , LLaVA-7B A , training image-text pairs $\mathbb{S} = \{\mathbb{I}, \mathbb{P}\}$.
- 2: **Offline Process:** Apply A to enrich the captions of \mathbb{S} , get $\hat{\mathbb{P}} = A(\mathbb{I})$ to replace the original \mathbb{P} .
- 3: \rightarrow **Begin Training.**
- 4: Freeze T_ϕ and T_L , training M and ϵ .
- 5: **while** L_{simple} not converged **do**
- 6: Sample p from \mathbb{P} ; $t = T$
- 7: $' \approx M(T_\phi(p), T_L(p))$ using Eq. (7).
- 8: Calculate L_{simple} using Eq. (9).
- 9: Backward L_{simple} and update ϵ, M .
- 10: **end while**
- 11: \rightarrow **End Training.**

the latent vectors on text embeddings. Notably, our LLM4GEN is compatible with both decoder-only and encoder-only LLMs and we evaluate on Llama-2 7B/13B [50] and T5-XL [4] in further experiments.

3.2.3 Training Objectives. Based on the framework described above, the training loss of LLM4GEN is formulated as:

$$L_{\text{simple}} = \mathbb{E}_{\mathbf{x}_0, \epsilon, \mathbf{c}_t, \mathbf{c}_l, t} \|\epsilon - \epsilon_\theta(\mathbf{x}_t, \mathbf{c}_t, \mathbf{c}_l, t)\|^2 \quad (9)$$

Besides, we randomly drop text embedding conditions in the training stage to enable classifier-free guidance in the inference stage:

$$\hat{\epsilon}_{\theta}(\mathbf{x}_t, \mathbf{c}_t, \mathbf{c}_l, t) = \omega \epsilon_{\theta}(\mathbf{x}_t, \mathbf{c}_t, \mathbf{c}_l, t) + (1 - \omega) \epsilon_{\theta}(\mathbf{x}_t, t) \quad (10)$$

The proposed LLM4GEN is further illustrated in Algorithm 2.

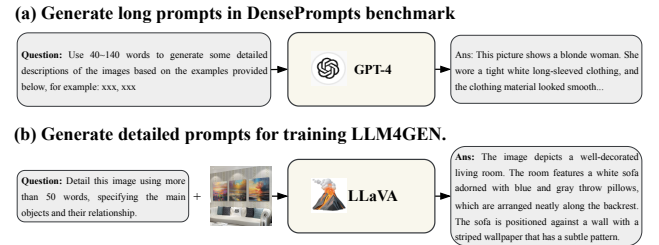


Figure 4: Pipeline of data construction. (a) The construction of DensePrompts benchmark. (b) The construction of the training dataset. We use GPT-4 [1] and LLaVA [25] as the caption models, respectively.

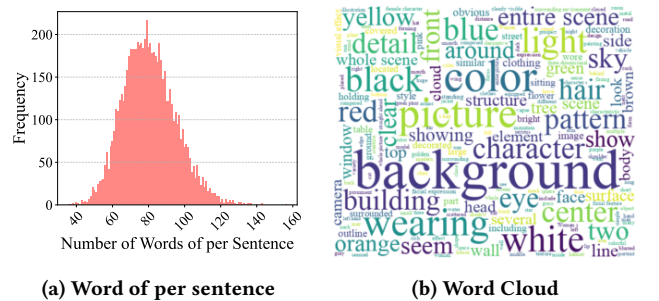


Figure 5: Statistic of DensePrompts benchmark.

4 DATASET CONSTRUCTION

4.1 DensePrompts Benchmark

A comprehensive benchmark is crucial for evaluating the image-text alignment of generated images. Current benchmarks, e.g., MSCOCO [24] and T2I-CompBench [16], primarily consist of concise textual

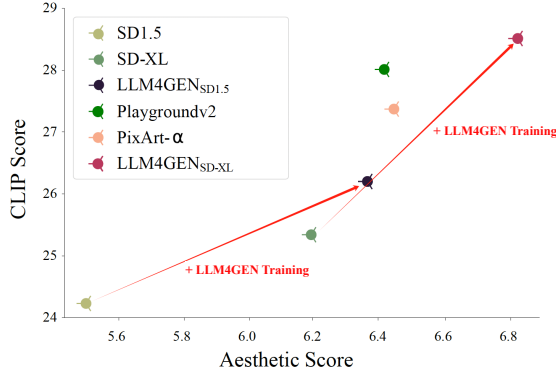


Figure 6: Aesthetic Score and CLIP Score (%) on DensePrompts benchmark.

descriptions, are not comprehensive enough to describe a diverse range of objects. Thus, we introduce a new comprehensive and complicated benchmark called **DensePrompts**, comprising lengthy textual descriptions.

Initially, we collect 100 images from the Internet, comprising 50 real and 50 generated images, each with intricate details. Leveraging the robust image comprehension capabilities of GPT-4V [29], we utilize it to provide detailed descriptions for these 100 images, encompassing object attributes and their relationships, thereby generating comprehensive prompts abundant in semantic details. As depicted in Fig. 4 (a), we employ GPT-4 [1] to produce massive long texts based on generated prompts mentioned above. DensePrompts provides more than 7,000 extensive prompts whose average word length is more than 40. Word statistics of DensePrompts are outlined in Fig. 5. To assess the performance, DensePrompts benchmark incorporates CLIP Score [32] and Aesthetic Score [41]. Combining our proposed DensePrompts with T2I-CompBench, we establish a comprehensive evaluation in text-to-image generation.

4.2 Training Dataset Construction

Current text-to-image diffusion models use text-image pairs collected from the Internet, where the text descriptions are often brief and disconnected. This leads to a weak correlation between images and text, limited dense semantic information, and necessitates a large number of image-text pairs for model convergence.

In this paper, we propose a 1M LAION-refined dataset, including the refined image descriptions of the open-source LAION [42] dataset. We select 1M images from LAION [42] with an aesthetic score [41] exceeding 6.5, a minimum short edge resolution of 512 pixels, and a maximum aspect ratio of 1.5. We utilize LLaVA-7B [25] to generate dense and highly descriptive captions for each image. The process of dataset construction is illustrated in Fig. 4 (b).

5 EXPERIMENTS

5.1 Experimental Details

Framework. In this paper, we explore LLM4GEN based on SD1.5 [35] and SDXL [31], denoted as LLM4GEN_{SD1.5} and LLM4GEN_{SDXL}. We utilize T5-XL [33] and CLIP text encoder as the text tower. The

sequence length of the LLMs is set to 128, enhancing the representation of conditional text embedding.

Implementation Details. We employ AdamW [27] optimizer to train our models. The learning rates are set to 2e-5 and 1e-5 for LLM4GEN_{SD1.5} and LLM4GEN_{SDXL}, respectively. The batch size is set to 256. The training steps are set to 20k and 40k. Additionally, we further train LLM4GEN_{SDXL} using 20K high-quality data with 1024 resolution. The final LLM4GEN_{SD1.5} model is trained on 8 80G A100 for 2 days while 4 days for LLM4GEN_{SDXL} model. During inference, we utilize DDIM sampler [44] for sampling, setting the number of time steps to 50 and the classifier free guidance scale to 7.5.

Evaluation Benchmarks. We comprehensively evaluate proposed LLM4GEN via four primary benchmarks:

- (1) **MSCOCO Dataset** [24] We randomly select 30k images from MSCOCO dataset and assess both sample quality and image-text alignment of generated images. The Fréchet Inception Distance (FID) [12], Inception Score (IS) [39], and CLIP Score [32] are used for evaluation.
- (2) **T2I-CompBench** [16] We employ various compositional prompts to assess textual attributes, including aspects such as color, shape, and texture, as well as attribute binding.
- (3) **DensePrompts** Our proposed benchmark involves extensive textual descriptions comprising over 7,000 dense prompts. The CLIP Score and Aesthetic Score are used for evaluation.
- (4) **User Study** We randomly select 100 prompts from our proposed DensePrompts benchmark and 100 prompts from T2I-CompBench. Subsequently, we enlist 20 participants for the user study.

5.2 Performance Comparisons and Analysis

5.2.1 Fidelity assessment on MSCOCO benchmark. Experimental results on MSCOCO benchmark are shown in Tab. 2. LLM4GEN notably enhances the sample quality and image-text alignment, resulting in improvements of 1.79 and 0.54 on FID compared to SD1.5 and SDXL, respectively. Furthermore, we assess the performance of SD1.5 after extensive fine-tuning with the same training dataset. This modified version, SD1.5 (ft), surpasses the original SD1.5, yet LLM4GEN_{SD1.5} still exhibits superior performance over SD1.5 (ft). This underscores the potent representation of our proposed LLM4GEN and its contribution to text-to-image generation.

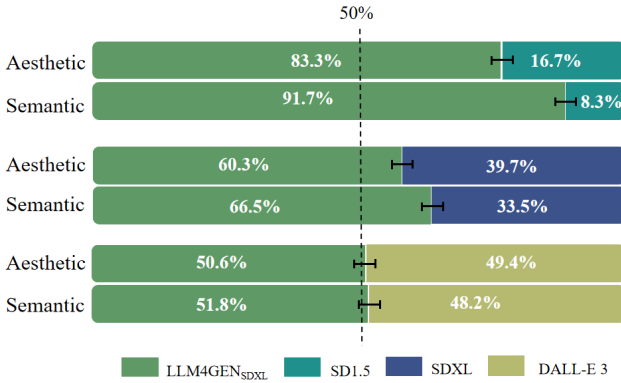
5.2.2 Evaluation on T2I-CompBench. For T2I-CompBench comparison, we select the recent text-to-image generative models for comparison, e.g., Composable Diffusion [26], Structured Diffusion [11], Attn-Exct v2 [6], GORS [16], DALLE 2 [34], PixArt-α [8], ELLA_{SDXL} [15], SD1.5[35], and SDXL[31]. Experimental results shown in Tab. 1 demonstrate the distinctive performance of LLM4GEN_{SDXL} in T2I-CompBench evaluation, underlining its advancements in attribute binding, object relationship, and mastery in rendering complex compositions. LLM4GEN shows considerable improvement in color, shape, and texture, showcasing enhancements up to +9.60% in color, +11.52% in texture, and +3.26% in shape with SDXL, respectively. LLM4GEN_{SDXL} also marks considerable progress in both spatial and non-spatial evaluations, with 2.27% and 0.84% lift, respectively. Furthermore, when compared with the recent PixArt-α, which employs T5-XL as its text encoder, LLM4GEN_{SDXL} surpasses it in

Table 1: Evaluation results (%) on T2I-CompBench [16]. The higher is better, and the best results are highlighted in bold.

Model	Attribute Binding			Object Relationship		Complex↑
	Color ↑	Shape ↑	Texture ↑	Spatial ↑	Non-Spatial ↑	
Composable Diffusion [26]	40.63	32.99	36.45	8.00	29.80	28.98
Structured Diffusion [11]	49.90	42.18	49.00	13.86	31.11	33.55
Attn-Exct v2 [6]	64.00	45.17	59.63	14.55	31.09	34.01
GORS [16]	66.03	47.85	62.87	18.15	31.93	33.28
DALL-E 2 [34]	57.50	54.64	63.74	12.83	30.43	36.96
PixArt- α [8]	68.86	55.82	70.44	20.82	31.79	41.17
ELLA _{SDXL} [15]	72.60	56.34	66.86	22.14	30.69	-
SD1.5 [35]	37.65	35.76	41.56	12.46	30.79	30.80
LLM4GEN _{SD1.5}	45.34	43.28	51.52	13.12	30.94	32.33
Δ (Margin)	+7.69	+7.52	+9.94	+0.66	+0.15	+1.53
SDXL [31]	63.69	54.08	56.37	20.32	31.10	40.91
LLM4GEN _{SDXL}	73.29	57.34	67.86	22.59	31.94	41.23
Δ (Margin)	+9.60	+3.26	+11.52	+2.27	+0.84	+0.33

Table 2: Quantitative comparison on text-to-image generation models on the subset of MSCOCO [24] dataset.

Method	FID↓	IS↑	CLIP Score(%)↑
SD1.5 [35]	26.89	32.24	28.66
SD1.5 (ft)	25.48	33.53	29.10
LLM4GEN _{SD1.5}	25.20	34.24	29.45
SDXL [31]	24.75	34.91	30.10
LLM4GEN _{SDXL}	24.21	35.10	30.91

**Figure 7: Results on user study regarding the sample quality and image-text alignment of different models.**

several aspects, such as a notable 3.43% lead in color metric. Moreover, LLM4GEN_{SDXL} outperforms ELLA_{SDXL}. These results verify the potent synergy of LLMs representations in augmenting the sample quality and image-text alignment of diffusion models.

5.2.3 Evaluation on DensePrompts. We compare our LLM4GEN with PixArt α [8], Playground v2 [19], SD1.5 [35], SDXL [31] on our designed DensePrompts benchmark. As illustrated in Fig. 6, LLM4GEN_{SDXL} stands out by achieving the highest scores in both Aesthetic Score and CLIP Score among these models. PixArt- α demonstrates superior results to SDXL, attributed to its use of the T5-XL text encoder for processing dense prompts. LLM4GEN demonstrates an exceptional ability to understand and interpret dense prompts, leading to generated images with high sample quality and image-text alignment. We attribute this performance improvement to the powerful representation of LLMs, which enables the effective adaptation of the original CLIP text encoder through the well-designed Cross-Adapter Module.

To thoroughly evaluate our proposed LLM4GEN framework, we present the qualitative results on the short prompts provided by PartiPrompts [57] in the first 4 columns and on the dense prompts provided by DensePrompts in the last 3 columns in Fig. 8. The results indicate that our proposed LLM4GEN_{SD1.5} and LLM4GEN_{SDXL} exhibit strong text-image alignment and superior dense prompt generation compared to the recent PixArt- α and Playground v2, especially in handling the multiple objects and attribute binding.

5.2.4 User Study. We conduct the user study on various combinations of existing methods and LLM4GEN_{SDXL}. For each pairing, we assess two criteria: sample quality and image-text alignment. Users are tasked with evaluating the aesthetic appeal and semantic understanding of images with identical text to determine the superior one based on these assessment criteria. Subsequently, we compute the percentage scores for each model, as shown in Fig. 7. The results showcase our LLM4GEN_{SDXL} exhibits comparative advantages over both SD1.5 and SDXL. Specifically, LLM4GEN_{SDXL} achieves 60.3% and 66.5% higher voting preferences compared to

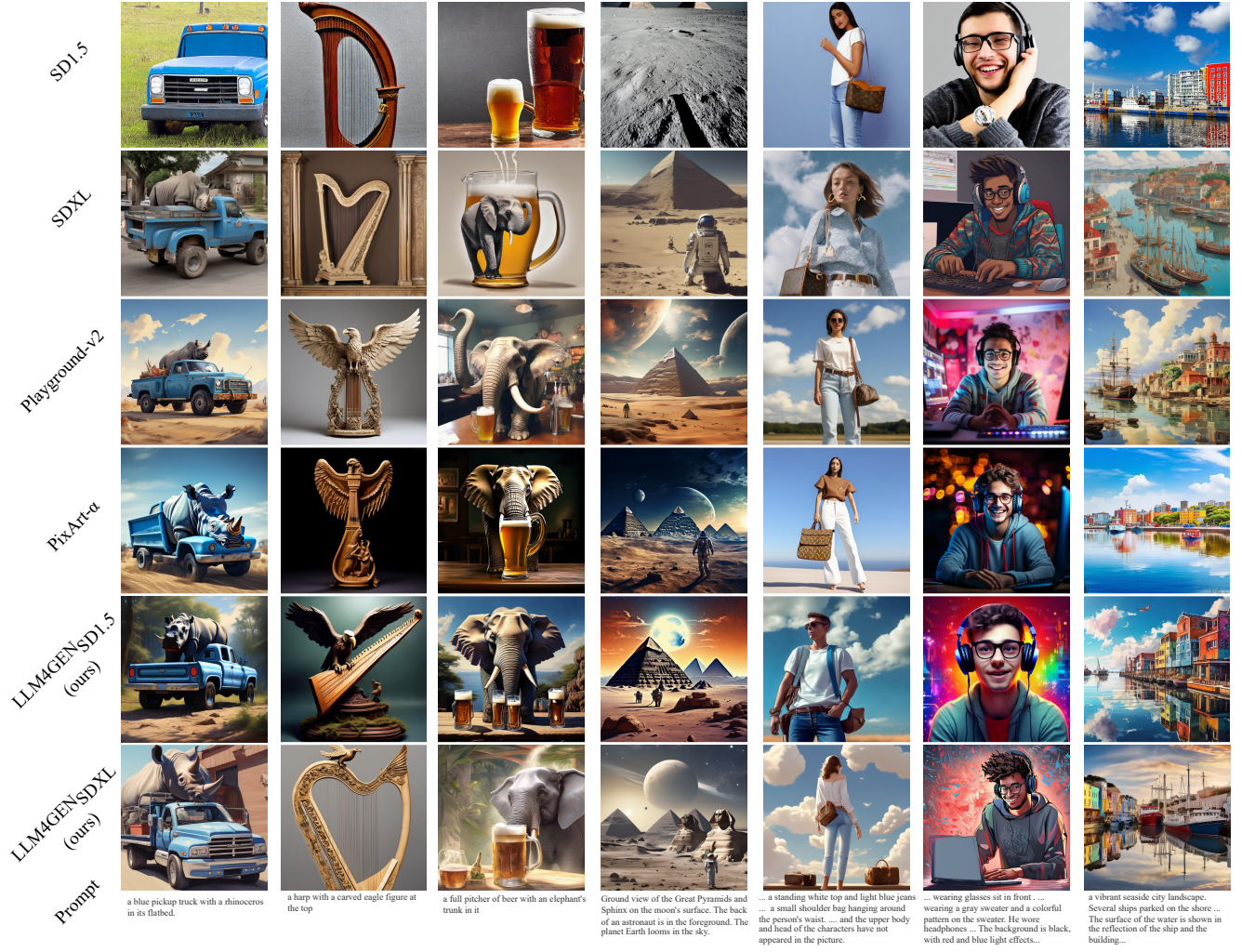


Figure 8: A comparative analysis of LLM4GEN and other state-of-the-art diffusion models using PartiPrompts [57] and our proposed DensePrompts as prompts. The last row represents the prompts used.

SDXL in terms of Aesthetic and Semantic, respectively. Notably, LLM4GEN_{SDXL} also delivers competitive results when compared to DALL-E 3.

Table 3: Impact (%) of the designed Cross-Adapter Module. The symbol \times denotes cases where the model fails to generate images without the original text encoder.

Module	Attribute Binding		
	Color \uparrow	Shape \uparrow	Texture \uparrow
(1) SD1.5 [35]	37.65	35.76	41.56
(2) MLP or CrossAttention	\times	\times	\times
(3) MLP + Concat	40.24	38.23	44.39
(4) CrossAttention + Concat	45.34	43.28	51.52

Table 4: Impact (%) of Different LLMs based on SD1.5.

LLMs	Attribute Binding		
	Color \uparrow	Shape \uparrow	Texture \uparrow
SD1.5 [35]	37.65	35.76	41.56
Llama-2/7B [50]	43.21	40.12	48.91
Llama-2/13B [50]	43.98	41.03	49.21
T5-XL [33]	45.34	43.28	51.52

5.3 Ablation Studies

Impact of Cross-Adapter Module. Due to limited computing sources, we evaluate the impact of various architectural enhancements on SD1.5, as outlined in Tab. 3. Our configurations explore different methods for integrating LLMs embeddings: (1) **the base-line SD1.5 model**, (2) **MLP or CrossAttention**, which utilizes a simple linear layer or cross-attention layer to transform LLM embeddings, (3) **MLP + Concat**, representing a process where LLMs embeddings are projected to the same dimension as the original

text embeddings before concatenation, and (4) **CrossAttention + Concat**, our innovative approach detailed in Sec. 3.2. Results show that configuration (2) is incapable of generating images from text, likely due to a misalignment between LLMs and the latent vector, necessitating substantial resources for alignment, as mentioned in [15] and [54]. Interestingly, simply concatenating the original text embeddings (configuration 3) provides a significant boost over base SD1.5, with a 2.59% improvement in color. This suggests that direct representation alignment between LLMs and the latent vector is challenging, and enhancing the original text embeddings with LLM embeddings is sufficient to improve image-text alignment. Furthermore, the result of our carefully crafted Cross-Adapter Module (configuration 4) achieves a 5.10% increase in color over configuration 3. This emphasizes the substantial benefits of incorporating our Cross-Adapter Module to enrich the representation of the original text encoder and the image-text alignment of generated images.

Table 5: Training resources comparison, including the scale of training data (#Images) and computing cost (#GPU days). The performance (%) is evaluated on the Color in T2I-CompBench.

Method	#Images (M ↓)	#GPU days (↓)	Performance (↑)
PixArt- α [8]	25	753	68.86
ParaDiffusion [54]	500	392	-
ELLA _{SDXL} [15]	30	112	72.60
LLM4GEN _{SDXL}	2	32	73.29

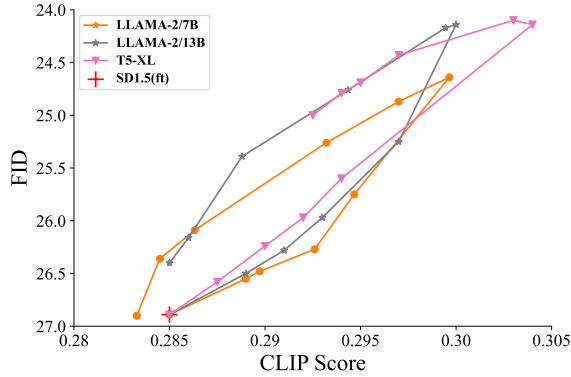


Figure 9: Performance metrics of LLM4GEN based on different LLMs across λ values from 0 to 2.

Impact of Different LLMs. The analysis encompasses a comparative evaluation between base SD1.5 and the enhancements achieved through the integration of Llama-2/7B, Llama-2/13B, and T5-XL. As depicted in Tab. 4, the inclusion of any LLM improves upon the performance of SD1.5. Importantly, Llama-v2/13B outperforms Llama-v2/7B, demonstrating that LLMs with greater capacity excel in extracting more nuanced semantic embeddings. Furthermore, when compared to decoder-only LLMs, T5-XL encoder demonstrates advantages in semantic comprehension, confirming its superior suitability for enhancing text-to-image generation.

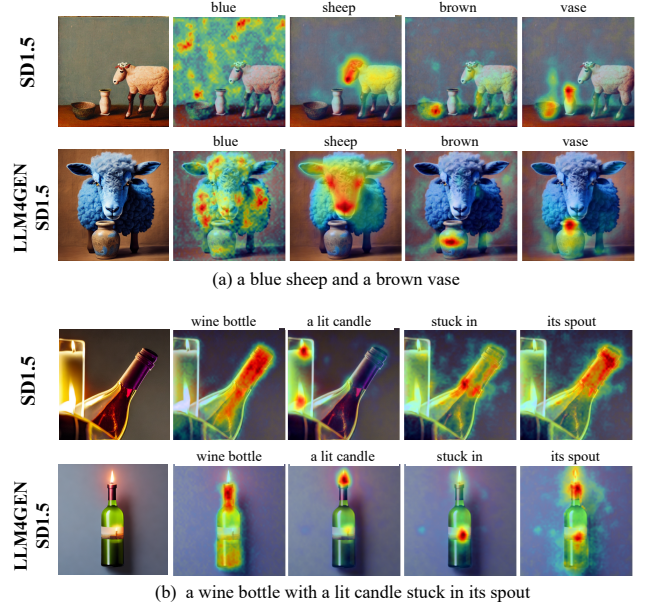


Figure 10: Cross-attention visualization [49] for two generated images. The two rows are SD1.5 and LLM4GEN_{SD1.5}, respectively.

Impact of hyperparameter λ . As depicted in Eq. (7), the hyperparameter λ is used to regulate the weight of the LLM’s embedding injected into the original text embedding. We evaluate the impact of λ in Fig. 9 with FID and CLIP Score for LLM4GEN_{SD1.5} on MSCOCO dataset across different LLMs. The λ varies from 0 to 2 in 0.2 increments. As the λ increases, we observe an initial enhancement in the model’s performance, followed by a slight decline. This pattern indicates that integrating LLMs representation into that of the original text encoder can consistently improve the image-text alignment beyond the capabilities of the original SD1.5, highlighting the beneficial impact of LLMs on semantic enrichment. However, setting higher values of λ does not lead to optimal performance, which we suspect stems from a misalignment between LLMs representation and the diffusion model. The best performance is achieved when λ is set to 1.0.

5.4 Further Analysis

Training Efficiency. When evaluating the effectiveness of integrating LLMs into text-to-image generation models, LLM4GEN_{SDXL} stands out for its remarkable efficiency and performance. LLM4GEN achieves significant reductions in both training data requirements and computational costs. It utilizes only 2M data, a 90% reduction compared to ELLA [15], and demands merely 32 GPU days for training, drastically lower than PixArt- α (25 million data, 753 GPU days) and ParaDiffusion (500 million data, 392 GPU days). Despite this, LLM4GEN_{SDXL} achieves a superior color metric performance of 73.29%. This notable difference underscores LLM4GEN’s ability to substantially reduce both training data and computational costs while establishing a new standard for performance efficiency.

Cross-attention Visualization. Fig. 10 demonstrates the cross-attention visualization [49] of SD1.5 and LLM4GEN_{SD1.5}, respectively. The heatmaps indicate that our proposed LLM4GEN method

exhibits a greater capacity to capture relationships between attributes, such as "blue" and "sheep", as illustrated in Fig. 10 (a). We attribute this capability to the enhanced semantic richness facilitated by the robust representation of LLMs.

More visualization and experimental results are shown in the Supplementary Materials.

6 CONCLUSION

In this paper, we propose LLM4GEN, an end-to-end text-to-image generation framework. Specifically, we design an efficient Cross-Adapter Module to leverage the powerful representation of LLMs to enhance the original text representation of diffusion models. Despite using fewer training data and computational resources, LLM4GEN outperforms current state-of-the-art text-to-image diffusion models in sample quality and image-text alignment. Additionally, we introduce LAION-refined dataset and DensePrompts benchmark, which promote generating images with dense information and establish a comprehensive evaluation, respectively. Furthermore, we aim to explore the potential of LLM4GEN within the transformer-based diffusion model. We hope this work will pave the way for new research directions in text-to-image generation and provide insights into how LLMs can contribute to improving the performance of text-to-image generation models.

REFERENCES

- [1] Josh Achiam, Steven Adler, Sandhini Agarwal, Lama Ahmad, Ilge Akkaya, Florencia Leoni Aleman, Diogo Almeida, Janko Altenschmidt, Sam Altman, Shyamal Anadkat, et al. 2023. Gpt-4 technical report. *arXiv preprint arXiv:2303.08774* (2023).
- [2] Jinze Bai, Shuai Bai, Shusheng Yang, Shijie Wang, Sinan Tan, Peng Wang, Junyang Lin, Chang Zhou, and Jingren Zhou. 2023. Qwen-vl: A frontier large vision-language model with versatile abilities. *arXiv preprint arXiv:2308.12966* (2023).
- [3] James Betker, Gabriel Goh, Li Jing, Tim Brooks, Jianfeng Wang, Linjie Li, Long Ouyang, Juntang Zhuang, Joyce Lee, Yufei Guo, et al. 2023. Improving image generation with better captions. *Computer Science*. <https://cdn.openai.com/papers/dall-e-3.pdf> (2023).
- [4] Tom B. Brown, Benjamin Mann, Nick Ryder, Melanie Subbiah, Jared Kaplan, Prafulla Dhariwal, Arvind Neelakantan, Pranav Shyam, Girish Sastry, Amanda Askell, Sandhini Agarwal, Ariel Herbert-Voss, Gretchen Krueger, Tom Henighan, Rewon Child, Aditya Ramesh, Daniel M. Ziegler, Jeffrey Wu, Clemens Winter, Christopher Hesse, Mark Chen, Eric Sigler, Mateusz Litwin, Scott Gray, Benjamin Chess, Jack Clark, Christopher Berner, Sam McCandlish, Alec Radford, Ilya Sutskever, and Dario Amodei. 2020. Language models are few-shot learners. *NeurIPS*.
- [5] Yupeng Chang, Xu Wang, Jindong Wang, Yuan Wu, Linyi Yang, Kaijie Zhu, Hao Chen, Xiaoyuan Yi, Cunxiang Wang, Yidong Wang, et al. 2023. A survey on evaluation of large language models. *ACM Transactions on Intelligent Systems and Technology* (2023).
- [6] Hila Chefer, Yuval Alaluf, Yael Vinker, Lior Wolf, and Daniel Cohen-Or. 2023. Attend-and-excite: Attention-based semantic guidance for text-to-image diffusion models. *ACM TOG* 42, 4 (2023), 1–10.
- [7] Jingwen Chen, Yingwei Pan, Ting Yao, and Tao Mei. 2023. Controlstyle: Text-driven stylized image generation using diffusion priors. In *ACM MM*. 7540–7548.
- [8] Junsong Chen, Jincheng Yu, Chongjian Ge, Lewei Yao, Enze Xie, Yue Wu, Zhongdao Wang, James Kwok, Ping Luo, Huchuan Lu, et al. 2023. PixArt- α : Fast Training of Diffusion Transformer for Photorealistic Text-to-Image Synthesis. *arXiv preprint arXiv:2310.00426* (2023).
- [9] Aakanksha Chowdhery, Sharan Narang, Jacob Devlin, Maarten Bosma, Gaurav Mishra, Adam Roberts, Paul Barham, Hyung Won Chung, Charles Sutton, Sebastian Gehrmann, et al. 2022. Palm: Scaling language modeling with pathways. *arXiv preprint arXiv:2204.02311* (2022).
- [10] Prafulla Dhariwal and Alexander Nichol. 2021. Diffusion models beat gans on image synthesis. In *NeurIPS*.
- [11] Weixi Feng, Xuehai He, Tsu-Jui Fu, Varun Jampani, Arjun Reddy Akula, Pradyumna Narayana, Sugato Basu, Xin Eric Wang, and William Yang Wang. 2022. Training-Free Structured Diffusion Guidance for Compositional Text-to-Image Synthesis. In *ICLR*.
- [12] Martin Heusel, Hubert Ramsauer, Thomas Unterthiner, Bernhard Nessler, and Sepp Hochreiter. 2017. Gans trained by a two time-scale update rule converge to a local nash equilibrium. In *NeurIPS*.
- [13] Jonathan Ho, Ajay Jain, and Pieter Abbeel. 2020. Denoising diffusion probabilistic models. *NeurIPS*.
- [14] Jonathan Ho and Tim Salimans. 2022. Classifier-free diffusion guidance. *arXiv preprint arXiv:2207.12598* (2022).
- [15] Xiwei Hu, Rui Wang, Yixiao Fang, Bin Fu, Pei Cheng, and Gang Yu. 2024. ELLA: Equip Diffusion Models with LLM for Enhanced Semantic Alignment. *arXiv preprint arXiv:2403.05135* (2024).
- [16] Kaiyi Huang, Kaiyue Sun, Enze Xie, Zhenguo Li, and Xihui Liu. 2023. T2I-CompBench: A Comprehensive Benchmark for Open-world Compositional Text-to-image Generation. In *ICCV*.
- [17] Rongjie Huang, Zhou Zhao, Huadai Liu, Jinglin Liu, Chenye Cui, and Yi Ren. 2022. Prodiff: Progressive fast diffusion model for high-quality text-to-speech. In *ACM MM*. 2595–2605.
- [18] Jing Yu Koh, Daniel Fried, and Russ R Salakhutdinov. 2023. Generating images with multimodal language models. In *NeurIPS*.
- [19] Daiqing Li, Aleks Kamko, Ali Sabet, Ehsan Akhgari, Linmiao Xu, and Suhail Doshi. [n. d.]. Playground v2. <https://huggingface.co/playgroundai/playground-v2-1024px-aesthetic>
- [20] Junnan Li, Dongxu Li, Silvio Savarese, and Steven Hoi. 2023. Blip-2: Bootstrapping language-image pre-training with frozen image encoders and large language models. In *ICML*.
- [21] Junnan Li, Dongxu Li, Caiming Xiong, and Steven Hoi. 2022. Blip: Bootstrapping language-image pre-training for unified vision-language understanding and generation. In *ICML*. 12888–12900.
- [22] Yuheng Li, Haotian Liu, Qingyang Wu, Fangzhou Mu, Jianwei Yang, Jianfeng Gao, Chunyuan Li, and Yong Jae Lee. 2023. Gligen: Open-set grounded text-to-image generation. In *CVPR*. 22511–22521.
- [23] Long Lian, Boyi Li, Adam Yala, and Trevor Darrell. 2024. LLM-grounded Diffusion: Enhancing Prompt Understanding of Text-to-Image Diffusion Models with Large Language Models. *Transactions on Machine Learning Research* (2024).
- [24] Tsung-Yi Lin, Michael Maire, Serge Belongie, James Hays, Pietro Perona, Deva Ramanan, Piotr Dollár, and C Lawrence Zitnick. 2014. Microsoft coco: Common objects in context. In *ECCV*.
- [25] Haotian Liu, Chunyuan Li, Qingyang Wu, and Yong Jae Lee. 2023. Visual instruction tuning. In *NeurIPS*.
- [26] Nan Liu, Shuang Li, Yilun Du, Antonio Torralba, and Joshua B Tenenbaum. 2022. Compositional visual generation with composable diffusion models. In *ECCV*. 423–439.
- [27] Ilya Loshchilov and Frank Hutter. 2017. Decoupled weight decay regularization. *arXiv preprint arXiv:1711.05101* (2017).
- [28] Alex Nichol, Prafulla Dhariwal, Aditya Ramesh, Pranav Shyam, Pamela Mishkin, Bob McGrew, Ilya Sutskever, and Mark Chen. 2022. Glide: Towards photorealistic image generation and editing with text-guided diffusion models. In *ICML*.
- [29] OpenAI. 2023. GPT-4V(ision) System Card. <https://api.semanticscholar.org/CorpusID:263218031>
- [30] Ziqi Pang, Ziyang Xie, Yunze Man, and Yu-Xiong Wang. 2024. Frozen transformers in language models are effective visual encoder layers. In *ICLR*.
- [31] Dustin Podell, Zion English, Kyle Lacey, Andreas Blattmann, Tim Dockhorn, Jonas Müller, Joe Penna, and Robin Rombach. 2023. Sdxl: Improving latent diffusion models for high-resolution image synthesis. *arXiv preprint arXiv:2307.01952* (2023).
- [32] Alec Radford, Jong Wook Kim, Chris Hallacy, Aditya Ramesh, Gabriel Goh, Sandhini Agarwal, Girish Sastry, Amanda Askell, Pamela Mishkin, Jack Clark, et al. 2021. Learning transferable visual models from natural language supervision. In *ICML*. 8748–8763.
- [33] Colin Raffel, Noam Shazeer, Adam Roberts, Katherine Lee, Sharan Narang, Michael Matena, Yanqi Zhou, Wei Li, and Peter J Liu. 2020. Exploring the limits of transfer learning with a unified text-to-text transformer. *JMLR* 21, 1 (2020), 5485–5551.
- [34] Aditya Ramesh, Prafulla Dhariwal, Alex Nichol, Casey Chu, and Mark Chen. 2022. Hierarchical text-conditional image generation with clip latents. *arXiv preprint arXiv:2204.06125* (2022).
- [35] Robin Rombach, Andreas Blattmann, Dominik Lorenz, Patrick Esser, and Björn Ommer. 2022. High-resolution image synthesis with latent diffusion models. In *CVPR*. 10684–10695.
- [36] Olaf Ronneberger, Philipp Fischer, and Thomas Brox. 2015. U-net: Convolutional networks for biomedical image segmentation. In *MICCAI*. 234–241.
- [37] Nataniel Ruiz, Yuanzhen Li, Varun Jampani, Yael Pritch, Michael Rubinstein, and Kfir Aberman. 2023. Dreambooth: Fine tuning text-to-image diffusion models for subject-driven generation. In *CVPR*. 22500–22510.
- [38] Chitwan Saharia, William Chan, Saurabh Saxena, Lala Li, Jay Whang, Emily L Denton, Kamyar Ghasemipour, Raphael Gontijo Lopes, Burcu Karagol Ayan, Tim Salimans, et al. 2022. Photorealistic text-to-image diffusion models with deep language understanding. In *NeurIPS*.

- [39] Tim Salimans, Ian Goodfellow, Wojciech Zaremba, Vicki Cheung, Alec Radford, and Xi Chen. 2016. Improved techniques for training gans. In *NeurIPS*.
- [40] Teven Le Scao, Angela Fan, Christopher Akiki, Ellie Pavlick, Suzana Ilić, Daniel Hesslow, Roman Castagné, Alexandra Sasha Luccioni, François Yvon, Matthias Galle, et al. 2022. Bloom: A 176b-parameter open-access multilingual language model. *arXiv preprint arXiv:2211.05100* (2022).
- [41] Christoph Schuhmann. [n.d.]. CLIP+MLP Aesthetic Score Predictor. <https://github.com/christophschuhmann/improved-aesthetic-predictor>.
- [42] Christoph Schuhmann, Richard Vencu, Romain Beaumont, Robert Kaczmarczyk, Clayton Mullis, Aarush Katta, Theo Coombes, Jenia Jitsev, and Aran Komatsuzaki. 2021. LAION-400M: Open Dataset of CLIP-Filtered 400 Million Image-Text Pairs. *CoRR abs/2111.02114* (2021). [arXiv:2111.02114](https://arxiv.org/abs/2111.02114) <https://arxiv.org/abs/2111.02114>
- [43] Jascha Sohl-Dickstein, Eric Weiss, Niru Maheswaranathan, and Surya Ganguli. 2015. Deep unsupervised learning using nonequilibrium thermodynamics. In *ICML*. 2256–2265.
- [44] Jiaming Song, Chenlin Meng, and Stefano Ermon. 2020. Denoising Diffusion Implicit Models. *CoRR abs/2010.02502* (2020). [arXiv:2010.02502](https://arxiv.org/abs/2010.02502) <https://arxiv.org/abs/2010.02502>
- [45] Yang Song and Stefano Ermon. 2019. Generative modeling by estimating gradients of the data distribution. *NeurIPS*.
- [46] Yang Song and Stefano Ermon. 2020. Improved techniques for training score-based generative models. *NeurIPS*.
- [47] Yang Song, Jascha Sohl-Dickstein, Diederik P Kingma, Abhishek Kumar, Stefano Ermon, and Ben Poole. 2020. Score-based generative modeling through stochastic differential equations. *arXiv preprint arXiv:2011.13456* (2020).
- [48] Quan Sun, Qiyang Yu, Yufeng Cui, Fan Zhang, Xiaosong Zhang, Yueze Wang, Hongcheng Gao, Jingjing Liu, Tiejun Huang, and Xinlong Wang. 2024. Emu: Generative pretraining in multimodality. In *ICLR*.
- [49] Raphael Tang, Linqing Liu, Akshat Pandey, Zhiying Jiang, Gefei Yang, Karun Kumar, Pontus Stenetorp, Jimmy Lin, and Ferhan Ture. 2022. What the daam: Interpreting stable diffusion using cross attention. *arXiv preprint arXiv:2210.04885* (2022).
- [50] Hugo Touvron, Louis Martin, Kevin Stone, Peter Albert, Amjad Almahairi, Yasmine Babaei, Nikolay Bashlykov, Soumya Batra, Prajjwal Bhargava, Shriti Bhosale, et al. 2023. Llama 2: Open foundation and fine-tuned chat models. *arXiv preprint arXiv:2307.09288* (2023).
- [51] Aaron Van Den Oord, Oriol Vinyals, et al. 2017. Neural discrete representation learning. In *NeurIPS*.
- [52] Ashish Vaswani, Noam Shazeer, Niki Parmar, Jakob Uszkoreit, Llion Jones, Aidan N Gomez, Łukasz Kaiser, and Illia Polosukhin. 2017. Attention is all you need. *NeurIPS*.
- [53] Shengqiong Wu, Hao Fei, Leigang Qu, Wei Ji, and Tat-Seng Chua. 2023. Next-gpt: Any-to-any multimodal llm. *arXiv preprint arXiv:2309.05519* (2023).
- [54] Weijia Wu, Zhuang Li, Yefei He, Mike Zheng Shou, Chunhua Shen, Lele Cheng, Yan Li, Tingting Gao, Di Zhang, and Zhongyuan Wang. 2023. Paragraph-to-image generation with information-enriched diffusion model. *arXiv preprint arXiv:2311.14284* (2023).
- [55] Ling Yang, Zhaochen Yu, Chenlin Meng, Minkai Xu, Stefano Ermon, and Bin Cui. 2024. Mastering text-to-image diffusion: Recaptioning, planning, and generating with multimodal llms. *arXiv preprint arXiv:2401.11708* (2024).
- [56] Ling Yang, Zhilong Zhang, Yang Song, Shenda Hong, Runsheng Xu, Yue Zhao, Wentao Zhang, Bin Cui, and Ming-Hsuan Yang. 2023. Diffusion models: A comprehensive survey of methods and applications. *Comput. Surveys* 56, 4 (2023), 1–39.
- [57] Jiahui Yu, Yuanzhong Xu, Jing Yu Koh, Thang Luong, Gunjan Baid, Zirui Wang, Vijay Vasudevan, Alexander Ku, Yinfei Yang, Burcu Karagol Ayan, et al. 2022. Scaling autoregressive models for content-rich text-to-image generation. *arXiv preprint arXiv:2206.10789* (2022).
- [58] Aohan Zeng, Xiao Liu, Zhengxiao Du, Zihan Wang, Hanyu Lai, Ming Ding, Zhuoyi Yang, et al. 2022. Glm-130b: An open bilingual pre-trained model. In *ICLR*.
- [59] Lvmin Zhang, Anyi Rao, and Maneesh Agrawala. 2023. Adding conditional control to text-to-image diffusion models. In *ICCV*.
- [60] Renrui Zhang, Jiaming Han, Aojun Zhou, Xiangfei Hu, Shilin Yan, Pan Lu, Hongsheng Li, Peng Gao, and Yu Qiao. 2024. Llama-adapter: Efficient fine-tuning of language models with zero-init attention. In *ICLR*.
- [61] Susan Zhang, Stephen Roller, Naman Goyal, Mikel Artetxe, Moya Chen, Shuohui Chen, Christopher Dewan, Mona Diab, Xian Li, Xi Victoria Lin, Todor Mihaylov, et al. 2022. Opt: Open pre-trained transformer language models. *arXiv preprint arXiv:2205.01068* (2022).
- [62] Deyao Zhu, Jun Chen, Xiaoqian Shen, Xiang Li, and Mohamed Elhoseiny. 2023. Minigpt-4: Enhancing vision-language understanding with advanced large language models. *arXiv preprint arXiv:2304.10592* (2023).

7 ADDITIONAL ANALYSIS

We provide the additional analysis and experimental results on our proposed LLM4GEN in the Supplementary Materials.

Formulation Derivation We provide a formula derivation of Eq. (8):

$$\begin{aligned}
 x &= \text{CA}(x, c'_t) \\
 &= \text{softmax} \left(Q' \cdot K'^T \right) \cdot V' \\
 &= \text{softmax} \left(W'_Q(x) \cdot W'_K(c'_t)^T \right) \cdot W'_V(c'_t) \\
 &= \text{softmax} \left(W'_Q(x) \cdot W'_K([\lambda \cdot c'_t, c_t]^T) \right) \cdot W'_V([\lambda \cdot c'_t, c_t]) \quad (11) \\
 &= \lambda \cdot \text{softmax} \left(W'_Q(x) \cdot W'_K(c'_t)^T \right) \cdot W'_V(c'_t) \\
 &\quad + \text{softmax} \left(W'_Q(x) \cdot W'_K(c_t)^T \right) \cdot W'_V(c_t) \\
 &= \lambda \cdot \text{CA}(x, c_t) + \text{CA}(x, c_t)
 \end{aligned}$$

where x denotes the latent noise, CA is the cross-attention module within the UNet module, which receives z as the query and c'_t as the key and value. And the W'_Q, W'_K, W'_V is the projector in the UNet. In this manner, the concatenation operation in Eq. (7) is equal to fuse the LLM-guided semantic feature to the latent noise for better text-to-image alignment.

Algorithm. The proposed LLM4GEN is further illustrated in Algorithm 2.

Algorithm 2 LLM4GEN Pipeline

- 1: **Input:** Pretrained UNet ϵ , pre-trained text encoder T_ϕ , pre-trained LLM T_L , Cross-Adapter Module M , LLaVA-7B A , training image-text pairs $\mathbb{S} = \{\mathbb{I}, \mathbb{P}\}$.
 - 2: **Offline Process:** Apply A to enrich the captions of \mathbb{S} , get $\hat{\mathbb{P}} = A(\mathbb{I})$ to replace the original \mathbb{P} .
 - 3: \rightarrow **Begin Training.**
 - 4: Freeze T_ϕ and T_L , training M and ϵ .
 - 5: **while** L_{simple} not converged **do**
 - 6: Sample p from \mathbb{P} ; $t = T$
 - 7: $c'_t = M(T_\phi(p), T_L(p))$ using Eq. (7).
 - 8: Calculate L_{simple} using Eq. (9).
 - 9: Backward L_{simple} and update ϵ, M .
 - 10: **end while**
 - 11: \rightarrow **End Training.**
-

8 ADDITIONAL EXPERIMENTAL RESULTS

Comparison with ParaDiffusion based on dense prompts. To further compare the proposed LLM4GEN with ParamDiffusion, we take three prompts provided in [54], and generate images using our LLM4GEN_{SD1.5} and LLM4GEN_{SDXL}. We select the generation images of ParaDiffusion from the original literature [54]. The results demonstrate that our proposed LLM4GEN can generate semantic-alignment images based on long textual descriptions and alleviate bad cases in ParaDiffusion, such as confusion between character generation and background in Fig. 11 (c). LLM4GEN_{SD1.5} even can generate high-quality and dense prompts alignment images than SDXL[31], such as Fig. 11 (b). It demonstrates our proposed

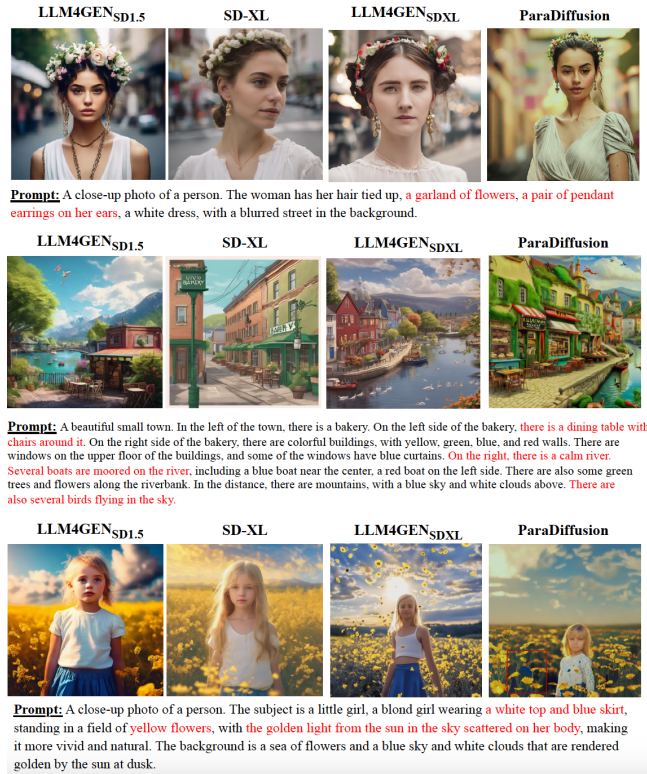


Figure 11: Comparison with ParaDiffusion [54]. The generation images of ParaDiffusion are from the original paper.



Figure 12: Comparison with ELLA [15]. The generation images of ParaDiffusion are from the original paper.

methods can efficiently integrate strong semantic representations of LLMs into text-to-image diffusion models to enhance image-text alignment.

Comparison with ELLA [15]. ELLA [15] also utilizes LLMs for text-to-image generation, with the aim of aligning LLMs with diffusion models from scratch, incurring significant training costs. In contrast to ELLA, our proposed LLM4GEN enhances the original text encoder directly with robust LLM semantic embeddings. This approach benefits from the powerful capabilities of LLM without high-cost training and computing sources. Compared to ELLA_{SDXL}, our model requires only 10% of the training data, but still produces high-quality images using the prompts provided in [15]. The visualization comparison is presented in Fig. 12.



Figure 13: LLM4GEN_{SD1.5} can be integrated with ControlNet [59] to generate images with guided poses.

Compatible with ControlNet [59]. We apply LLM4GEN with ControlNet [59], as shown in Fig. 13. We can see that LLM4GEN_{SD1.5} can be integrated with existing guided tools like ControlNet. LLM4GEN_{SD1.5} can be compatible with these standard methods while generates more consistent and text-align images.